Observation of oscillatory energy exchange in a coupled-atom–cavity system

R. J. Brecha,* L. A. Orozco,† M. G. Raizen, Min Xiao,‡ and H. J. Kimble§

Department of Physics, University of Texas at Austin, Austin, Texas 78712

Received November 11, 1994; revised manuscript received July 12, 1995

Observations of the oscillatory exchange of excitation between N two-state atoms and a single mode of a high-finesse optical cavity are reported in a regime of weak-field excitation and of comparable atomic and cavity damping rates. The observed frequencies of oscillation, approximately given by $g\sqrt{N}$, where g is the single-photon Rabi frequency, are in reasonable agreement with theoretical predictions. © 1995 Optical Society of America

1. INTRODUCTION

In recent years a great deal of attention has been focused on the study of the interaction of one atom or of a small collection of atoms with a single mode of a resonant cavity.[1–4] The boundary conditions associated with the cavity may lead to substantial modifications of the radiative processes relative to those encountered in free-space emission and absorption. The presence of the cavity mode enhances the coupling between the atoms and the electromagnetic field. In particular, if the coupling of the collective atomic polarization to the intracavity field is sufficiently strong compared with relevant dissipative processes, an oscillatory regime is encountered in which the field radiated by the atoms excites the cavity mode, which subsequently reexcites the atomic polarization, and so on. The origin of this oscillatory exchange between the atoms and the cavity can be understood simply in terms of a mode splitting for a coupled system of oscillators, with the normal modes of the composite system split by the exchange frequency $g\sqrt{N}$. Here g is the effective coupling coefficient for any one of the N atoms to the cavity field.

Several early experimental investigations of such phenomena used Rydberg atoms in microwave cavities.[5–10] In particular, the experiment of Kaluzny *et al.*[5] is of relevance to present work. That group reported for the first time the exchange of energy between atoms and field. Specifically, they prepared the polarization of the collection of atoms such that initially all the energy in the coupled oscillator pair was with the atomic oscillator. They then observed the time-dependent exchange of energy between the atoms and the cavity field. In this paper we report observations of this splitting in the optical regime that we made by monitoring the transient response of a collection of weakly excited atoms in a resonant optical interferometer.[11–14] Here we begin with the initial excitation in the field and the atoms in an unexcited state. An abrupt change in magnitude of the excitation field leads to an oscillatory regression to a new steady state, with the time evolution governed by the eigenvalues of the linearized Maxwell–Bloch equations. Although most often in optical physics the coupling frequency $g\sqrt{N}$ is small and is overshadowed by both the size and the disparity of the decay rates of the cavity field κ, of the atomic polarization $\gamma_\perp$, and of the atomic inversion γ, it was first demonstrated in Ref. 10 that the condition $g\sqrt{N} \gg (\kappa, \gamma_\perp, \gamma)$ can be readily achieved in the optical domain. In qualitative terms, the exchange of excitation is best observed when the dissipative rates of the cavity (κ) and the atoms ($\gamma_\perp$, γ) are comparable. However, it is still necessary to have $g\sqrt{N} > \gamma, \kappa$.

Because the interaction coupling $g\sqrt{N}$ is at the heart of this simple quantum optical system, its consequences go well beyond our observation of the "oscillatory regime of spontaneous emission"[5] reported here. In a similar system the spectrum of this coupled system has also been investigated by the use of a weak probe beam and a heterodyne detection scheme.[15–17] A two-peaked spectrum that corresponded to the response of the coupled system at frequencies $\pm g\sqrt{N}$ offset from the resonant frequency of the uncoupled atom or cavity-mode subsystems was observed. It was even possible to observe a splitting that was due to a single atom in the cavity. Furthermore, this same mode splitting was employed to generate squeezed states of light.[18,19] Subsequent to the above-mentioned observations of phenomena related to the so-called vacuum Rabi splitting, other investigations were undertaken as well.[20]

Evidence of the energy-exchange frequency also appears when one looks at the photon statistics of the light transmitted by a cavity strongly coupled to a small number of atoms; the photons emitted from the coupled system show the nonclassical property of photon antibunching, and in the time dependence of the correlations, an oscillatory behavior that corresponds exactly to this normal mode splitting is observed.[21]

This paper is organized as follows. In Section 2 we present the theory for the transient response of the atoms when they are coupled strongly to the cavity field. The results are cast into a form suitable for the description of the experiments. Experimental results for two different configurations are presented and discussed in Section 3, with each one showing a different aspect of the coupled N atom + cavity system.

0740-3224/95/122329-10$06.00

2. THEORY OF TRANSIENT RESPONSE

The model Hamiltonian for the interaction of a collection of N two-state atoms of transition frequency ω_a with a nearby single mode of a high-finesse interferometer of resonance frequency ω_c has been extensively studied in quantum optics. Our own work has its origins in the context of the optical bistability literature,[22,23] in which, in addition to the coherent cavity coupling characterized by the rate g, each atom is coupled to free-space modes, leading to damping rates $\gamma_\perp$ for the polarization and γ for the inversion, and for which the cavity field likewise decays to a continuum of free-space modes with rate κ.[21] Note that $(\gamma_\perp, \gamma)$ in general may differ from the usual free-space atomic decay rates in that those modes associated with the resonator are not included in the usual Weisskopf–Wigner treatment. For our particular experimental configuration, which is discussed below, the fraction of 4π sr subtended by the cavity mode is negligible. The Hamiltonian for the reversible coupling of the atoms and cavity is of the form

$$\hat{H} = \hat{H}_0 + \hat{H}_a + \hat{H}_c \tag{1}$$

$$= i\hbar g[\hat{J}_- \hat{a}^\dagger + \hat{a}\hat{J}_+] + (\hbar\omega_a/2)\hat{J}_z + \hbar\omega_c \hat{a}^\dagger \hat{a}\,. \tag{2}$$

The coherent coupling of the atomic polarization to the cavity field is described by $\hat{H}_0$. $(\hat{J}_z, \hat{J}_\pm)$ are collective atomic operators for the N atoms of transition frequency ω_a, and $(\hat{a}, \hat{a}^\dagger)$ are the annihilation and the creation operators, respectively, for the single cavity mode of resonant frequency ω_c.[22] The atoms and the cavity field are coupled through an assumed dipole interaction with coupling coefficient $g = (\omega_c {\mu_d}^2/2\hbar\epsilon_0 V_c)^{1/2}$, where μ_d is the transition dipole moment and V_c is the effective cavity-mode volume. The rotating wave approximation has been made to arrive at the above interaction part of the Hamiltonian.

In addition to the coherent processes described by $\hat{H}$, it is necessary to take into account spontaneous emission of the atoms to modes other than the cavity (at a rate γ), atomic polarization decay (rate $\gamma_\perp$), and loss of the cavity field through the mirrors (rate κ) that is due to coupling to a set of continuum input–output modes. Finally, the possibility of exciting the system with an external field y is considered as well. All these features can be handled by standard master equation techniques.[23]

In the limit $N \gg 1$, equations of motion for generalized quasiprobability distributions have been previously derived in the optical bistability literature.[22–24] The equations below for the mean values of the intracavity field $x = \langle\hat{a}\rangle/\sqrt{n_0}$ with $n_0 = \gamma\gamma_\perp/4g^2$, the atomic polarization $v = \langle\hat{J}\rangle/\sqrt{N}$, and atomic inversion $m = \langle\hat{J}_z\rangle/N$, are equivalent to the semiclassical Maxwell–Bloch equations, in which the intracavity field is self-consistently coupled to the atomic variables. Note that n_0 expresses the ratio of bad (i.e., dissipative) coupling into the vacuum modes compared with good (i.e., reversible) coupling into the cavity mode. Excitation is provided by an external driving field $y(t)$. For the weak-field limit for which $|x| \ll 1$, these equations become[22]

$$\frac{\mathrm{d}x}{\mathrm{d}\tau} = -\frac{\mu}{2}(1 + i\Theta)x + \frac{\mu C}{\sqrt{\Gamma}}v + \frac{\mu}{2}y(\tau),$$
$$\frac{\mathrm{d}v}{\mathrm{d}\tau} = -\frac{1}{2\Gamma}(1 + i\Delta)v - \frac{1}{2\sqrt{\Gamma}}x,$$
$$\frac{\mathrm{d}m}{\mathrm{d}\tau} = -[m(\tau) + 1]. \tag{3}$$

The choice of normalization for x and y permits a straightforward interpretation. y is the intracavity field in the absence of atoms, and x the intracavity field in the presence of atoms, where $|x|^2$, $|y|^2$ express an intracavity photon number of units of n_0.

Equations (3) are written in a rotating frame of frequency ω_L, the frequency of the external driving field, and time is scaled in units of $\gamma^{-1}(\tau = \gamma\tau)$, $\mu = 2\kappa/\gamma$, and $\Gamma = \gamma/2\gamma_\perp$. The cavity and the atomic detunings are defined by $\Theta = (\omega_c - \omega_L)/\kappa$ and $\Delta = (\omega_a - \omega_L)/\gamma_\perp$, respectively. The cooperativity parameter $C = g^2N/2\gamma_\perp\kappa$. Note that C has an interesting interpretation as being the ratio of coupling internal to the system (g^2) to the coupling to the outside world $(\gamma\kappa)$ for a single atom, multiplied by the number of atoms. In experimentally measurable terms, C is simply half the ratio of atomic loss to cavity loss, i.e., $C = \alpha l\mathcal{F}/2\pi$, where αl is the small-signal atomic absorption for $(\Delta = 0)$ and $\mathcal{F}$ is the cavity finesse. This definition of C originates in the optical bistability literature and was used to describe experiments for $N \gg 1$. More recent work,[17,21] in which $N \sim 1$, can still make use of the parameter C, but the definition in terms of an absorptive path length αl is perhaps not as useful a concept. However, a generalization of the definition of C was used in Ref. 20 to take into account (by the use of Monte Carlo simulation methods) the different coupling strengths for atoms located at various positions in the cavity mode.

It is apparent from Eqs. (3) that in the weak-field limit $(x \ll 1)$ the atomic polarization and the field mode of the cavity behave as linear, coupled oscillators. The atomic inversion is given to lowest order in x as simply $m(\tau) = -1$, independent of time. For the case $\Theta = \Delta = 0$, the eigenvalues found from Eqs. (3) for the normal mode frequencies associated with (v, x) are $\lambda_\pm/\gamma = -1/4(\mu + 1/\Gamma) \pm i\Omega$, where $\Omega = [\mu C/2\Gamma - (\mu - 1/\Gamma)^2/16]^{1/2}$. In unscaled time units this becomes $\lambda_\pm(\kappa + \gamma_\perp)/2\{[(\kappa - \gamma_\perp)/2]^2 - g^2N\}^{1/2}$. For the particular choice of equal cavity and polarization decay rates, we have $\lambda_\pm = (\kappa + \gamma_\perp)/2 \pm ig\sqrt{N}$. More generally, the exchange will be oscillatory when $g\sqrt{N}$ is larger than the difference between the cavity and the atomic polarization decay rates and will be resolvable if $g\sqrt{n}$ is greater than one-half the sum of the dissipative rates. The exchange of excitation will nevertheless decay at the average rate of the composite system. Although our analysis is for the case $N \gg 1$, in fact the splitting $g\sqrt{N}$ persists to the level $N = 1$ for[17] $x \ll 1$ and is a characteristic feature of the coherent interaction term in the parent Hamiltonian common to a wide range of problems in quantum optics.[1–4]

Because the eigenfunctions $u_\pm$ that correspond to the eigenvalues $\lambda_\pm$ are superpositions of both the cavity field x and the atomic polarization v, one is led to a perspective that views the atom–cavity interaction in terms of the dynamics of one composite system and not in terms of a simple redressing of atomic radiative processes. Only in the limit $\mu \to \infty(\kappa \gg \gamma)$ with C fixed can the field vari-

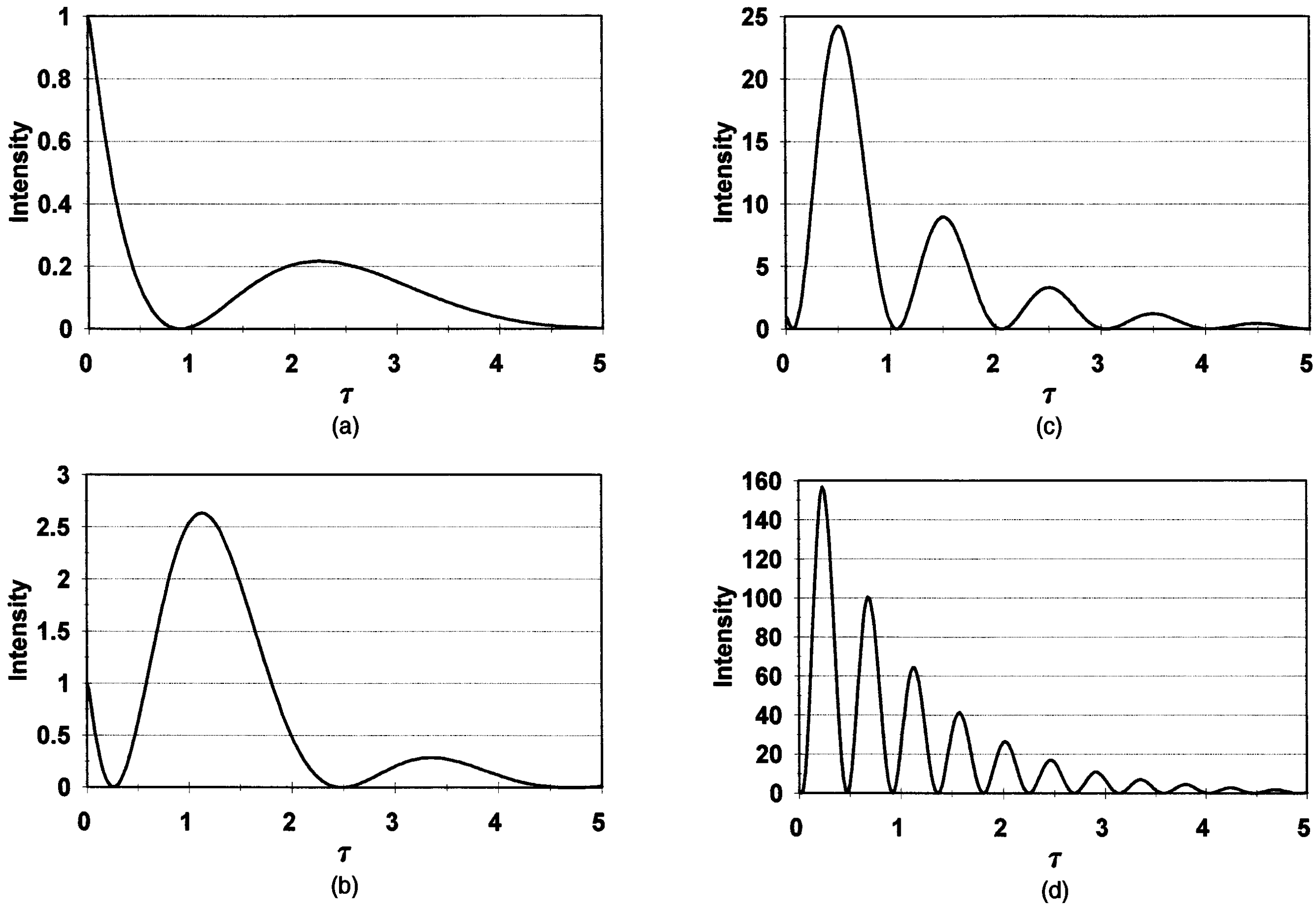

Fig. 1. Dependence of the oscillatory decay on the number of atoms in the cavity, which is proportional to the parameter C (see text). For (a)–(d), $\mu = 1$, the detunings are $\Delta = \Theta = 0$, $\alpha = 0$ (input field turns off completely), and $a = 0$ (input field turns off instantaneously). (a) $C = 1$, (b) $C = 4$, (c) $C = 20$, (d) $C = 100$.

ables be adiabatically eliminated to produce a description of enhanced or inhibited spontaneous emission and of radiative frequency shifts without references to the dynamical partnership between cavity and atoms. [Note that in this limit $\lambda = \gamma(1 + 2C)$, which is precisely the enhanced emission rate first noted by Purcell.[24]

Our current investigation centers on the time evolution of the intracavity field x (and hence of the transmitted field that is proportional to x) for a variation of the incident driving field $y(\tau)$. We choose $y(\tau)$ to be of the form

$$\begin{aligned} y(\tau) &= y_1, \qquad \tau < 0 \\ &= (y_1 - y_2)\exp(-a\tau) + y_2, \qquad \tau > 0, \end{aligned} \tag{4}$$

that is, the driving field $y(\tau)$ is switched from a constant value y_1 that has been maintained over the indefinite past to a new constant value y_2 that will be maintained in the indefinite future with an exponential transition of time constant a^{-1} (in units of γ^{-1}). Note that y_j corresponds to a steady-state value x_j, through Eqs. (3), with

$$y_j = \left[\left(1 + \frac{2C}{1+\Delta^2}\right) + i\left(\Theta - \frac{2C\Delta}{1+\Delta^2}\right)\right]x_j, \qquad j = 1, 2, \tag{5}$$

where y_j is constrained such that $|x_j| \ll 1$. Equation (5) is simply the state equation of optical bistability in the weak-field limit.[22]

Equations (3) can be solved for $x(\tau)$, given the assumed form for $y(\tau)$ from Eq. (4) in a straightforward fashion by Laplace transformation.[26] We find

$$\left|\frac{x(\tau)}{x(0)}\right| = \left| A_1 \exp\left(-\frac{b}{2}\tau\right)\sin\Omega\tau + A_2 \exp\left(-\frac{b}{2}\tau\right) \times \cos\Omega\tau + A_3\exp(-a\tau) + A_4\right|, \tag{6}$$

where the coefficients A_1, A_2, A_3, and A_4 are functions of μ, C, a, Δ, Θ, and $\alpha = y_2/y_1$, and are given by

$$\begin{aligned} A_1 \equiv &-\frac{\mu C(1 - i\Delta)}{(1+\Delta^2)\Omega} \\ &- \frac{1}{\Omega}\left[\frac{1}{4}\left(\mu - \frac{1}{\Gamma}\right) + \frac{i}{4}\left(\mu\Theta - \frac{\Delta}{\Gamma}\right)\right] + \frac{d\alpha}{2\Omega} \\ &\times \left[\mu - \frac{(1+i\Delta)b}{(1+2C) - \Delta\Theta + i(\Delta + \Theta)}\right] \\ &+ \frac{\mu d(1-\alpha)}{(b-2a)^2 + 4\Omega^2} \\ &\times \left\{2\Omega + \frac{(b-2a)}{\Omega}\left[\frac{1}{4}\left(\mu - \frac{1}{\Gamma}\right) + \frac{i}{4}\left(\mu\Theta - \frac{\Delta}{\Gamma}\right)\right]\right\}, \end{aligned}$$

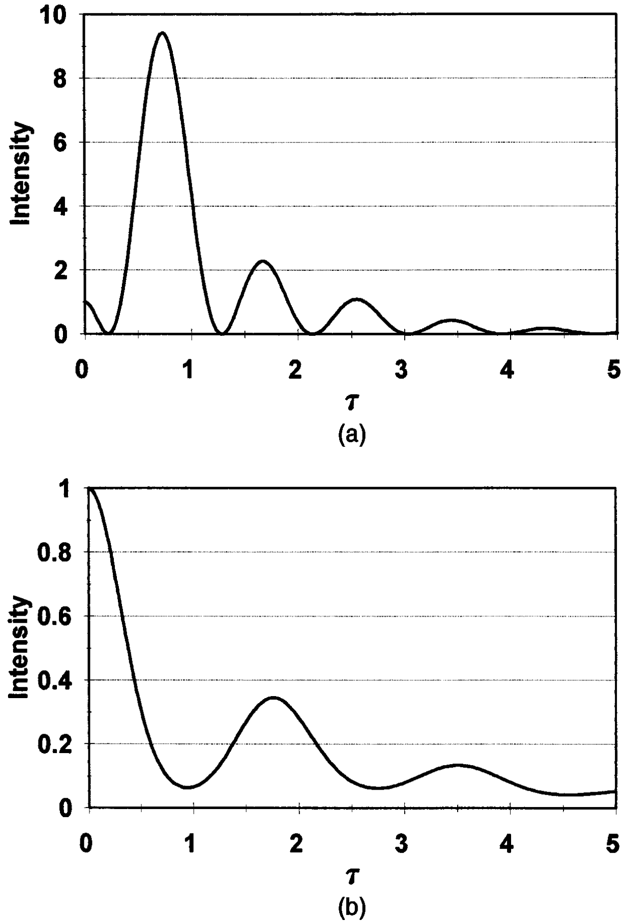

Fig. 2. Dependence of the oscillatory decay on a, the turnoff rate of the input field (see text). For both (a) and (b), $C = 50$, $\mu = 1$, and the detunings are $\Delta = \Theta = 0$, $\alpha = 0$ (input field turns off completely). (a) $a = 2$, (b) $a = 0.2$.

$$A_2 \equiv 1 - \frac{\alpha d(1 + i\Delta)}{(1 + 2C) - \Delta\Theta + i(\Delta + \Theta)} - \frac{\mu d(1 - \alpha)}{(b - 2a)^2 + 4\Omega^2}\left[\frac{(1 + i\Delta)}{\Gamma} - 2a\right],$$

$$A_3 \equiv \frac{\mu d(1 - \alpha)}{(b - 2a)^2 + 4\Omega^2}\left[\frac{(1 + i\Delta)}{\Gamma} - 2a\right],$$

$$A_4 \equiv \frac{\alpha d(1 + i\Delta)}{(1 + 2C) - \Delta\Theta + i(\Delta + \Theta)},$$

with

$$b \equiv \frac{1}{2}\left(\mu + \frac{1}{\Gamma}\right) + \frac{i}{2}\left(\mu\Theta + \frac{\Delta}{\Gamma}\right),$$

$$d \equiv \left(1 + \frac{2C}{1 + \Delta^2}\right) + i\left(\Theta - \frac{2C\Delta}{1 + \Delta^2}\right),$$

$$\Omega \equiv \left[\frac{\mu C}{2\Gamma} - \frac{1}{16}\left(\mu - \frac{1}{\Gamma}\right)^2 + \frac{1}{16}\left(\mu\Theta - \frac{\Delta}{\Gamma}\right)^2 + \frac{i}{8}\left(\mu - \frac{1}{\Gamma}\right)\left(\frac{\Delta}{\Gamma} - \mu\Theta\right)\right]^{1/2}.$$

We note in particular the case $\Delta = \Theta = 0$ with $a \to \infty$ and $y_2 = 0$, which corresponds to a step input pulse $y(t)$ from an initial value of y_1 to a final value of 0, for which

$$x(\tau) = \exp\left(-\frac{b}{2}\tau\right) \times \left[\frac{1}{4\Omega}\left(\frac{1}{\Gamma} - \mu - 4\mu C\right)\sin \Omega\tau + \cos \Omega\tau\right]. \quad (7)$$

For comparable atomic and field decay rates ($\mu \sim 1$) and for $\gamma\sqrt{\mu C} = g\sqrt{N}$ that are sufficiently large, we find an oscillatory regression of $x(\tau)$ to the new steady state at the frequency $\Omega \simeq g\sqrt{N}$. Excitation is repeatedly transferred from the atomic polarization to the cavity field and back again. Also note that for either $\tau = 0$ or $\tau \to \infty$, Eq. (6) reduces to the steady-state relation (5), as it must. Further, for the case of weak coupling between atoms and cavity ($C \to 0$) and for a step input pulse from y_1 to y_2, we find the usual expression for the transient response of an empty cavity[27]:

$$x(\tau) = x_2 + (x_1 - x_2)\exp[-2(1 + i\Theta)\mu\tau], \quad (8)$$

where $y_j = x_j(1 + i\Theta)$.

The results expressed in Eq. (6) are illustrated in Fig. 1. The response of the cavity without atoms [Eq. (6) with $C = 0$, $\Theta = 0$ and a step function from y_1 to y_0 at

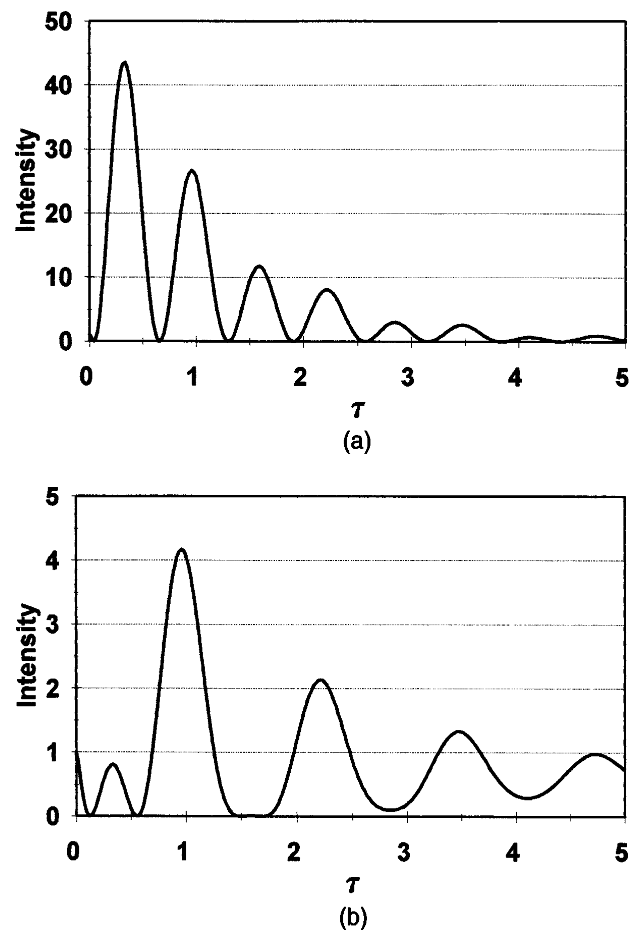

Fig. 3. Dependence of the oscillatory decay on α, the switching ratio of the input field (see text). Parameters are $C = 50$, $\mu = 1$, and the detunings are $\Delta = \Theta = 0$, $a = \infty$ (input field turns off infinitely fast). (a) $\alpha = 0.2$, (b) $\alpha = 0.8$.

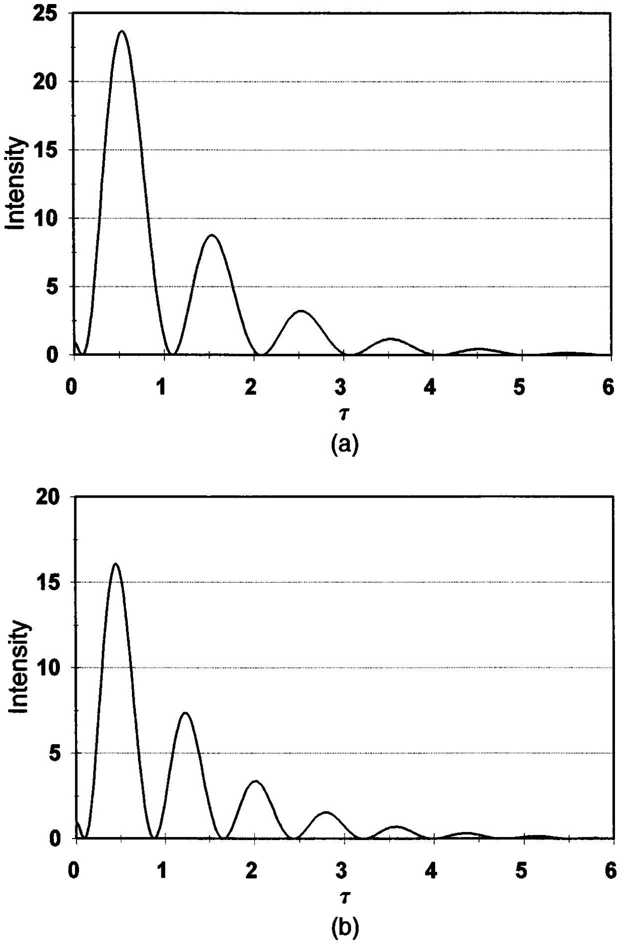

Fig. 4. Dependence of the oscillatory decay on Θ, the cavity detuning (see text). For both (a) and (b), $C = 20$, $\mu = 1$, and the detunings are $\Delta = 0$, $a = 0$, $\alpha \sim \infty$ (input field turns off infinitely fast). (a) $\Theta = 0$, (b) $\Theta = 10$.

$\tau = 0$] is simply an exponential decay at the rate 2κ (for the intensity). The change from monotonic decay at the rate 2κ to an oscillatory response that is characteristic of the coupled (atom plus field) system is rather striking. In Fig. 1 we consider Eq. (6) for increasing values of the cooperativity parameter C for $\mu = 2\kappa/\gamma = 1$. (This value of μ is chosen to correspond to that in experiments described in Section 3; the curves shown in Fig. 1 are quite insensitive to this choice for large C.) In addition to the coherent ringing shown in the figure, note that the initial value of the intracavity intensity $I(\tau) = |x(\tau)|^2$ becomes quite insignificant compared with the size of $I(\tau)$ at later times. This behavior can be easily understood in terms of the interference between the coherent driving field y and the field radiated by the atomic polarization. For $\Delta = \Theta = 0$ and for a step-function switching of $y(\tau)$ from y_1 to 0 at $\tau = 0$, we have from Eq. (5) that $x(0)_- = y_-/(1 + 2C)$, where the term $2C$ expresses the reduction of the intracavity field that is due to the atomic polarization. At time $\tau = 0_+$, just after the driving field has switched off but before the decay of the atomic polarization, the intracavity field $x(0_+) \simeq 2Cv \simeq -2Cy_-/(1 + 2C) \simeq -y_-$ for $C \gg 1$. Hence $x(0_+)/x(0_-) \simeq -2C$ and $I(0_+)/I(0_-) \simeq 4C^2$.

In qualitative terms, the driving field y and the field emitted by the polarization are similar in magnitude but are of opposite signs and hence interfere to produce a resultant field $|x| \ll y$. When y is switched off, the cavity field changes sign and is given by the polarization term alone. The excitation stored in the atomic polarization represents excitation of a superposition of normal modes; the decay is thus oscillatory at the frequency of the normal mode splitting. Note that because the peak emission intensity scales as N^2, the atomic emission is cooperative in the sense of superradiance, which is an analogy that has been repeatedly stressed in the literature on optical bistability. Indeed, in view of the discussion in Ref. 6, we might call this transient decay the ringing regime of superradiance without quantum fluctuations. For $N \gg 1$ quantum fluctuations play no role because the atomic polarization starts from a large nonzero value without the requirement of quantum initiation.

We explore the influence of a finite turnoff time a^{-1} for the incident field $y(\tau)$ in Figs. 2(a) and 2(b). For both cases, the cooperativity parameter $C = 50$, $\mu = 1.0$, $\Gamma = 1.0$, and $\Delta = \Theta = 0$. We change only the rate a at which the field y is reduced from y_1 to 0. Note that as the rate decreases, the prominent features displayed in Fig. 1, for which the rate of switching was assumed to be infinitely fast, are gradually lost. In this regard the following two time scales are relevant: (1) For $a \sim \sqrt{\mu C} \gg 1$, an appreciable fraction of the initial field y_1 is

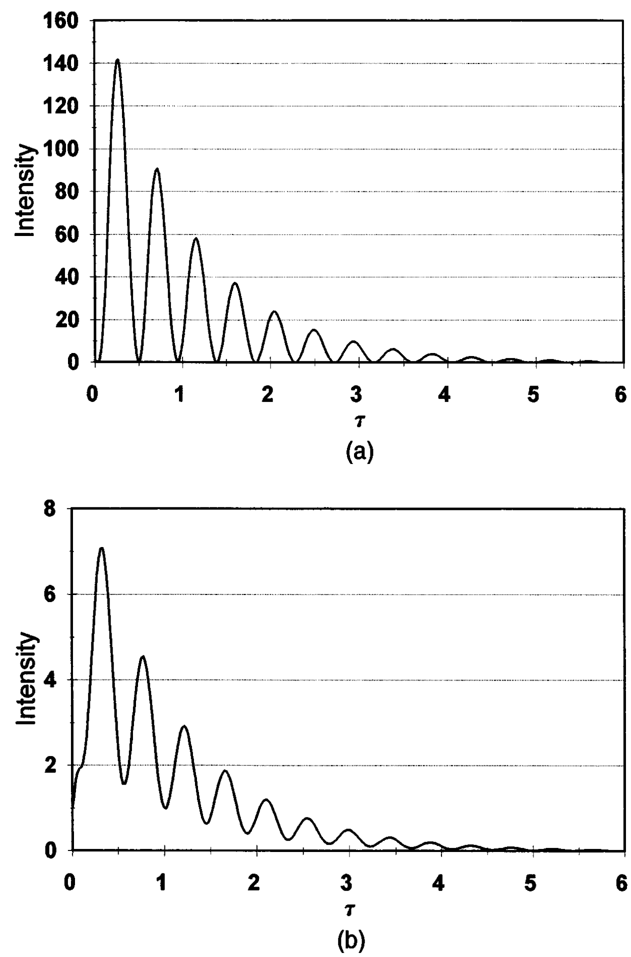

Fig. 5. Dependence of the oscillatory decay on Δ, the atomic detuning (see text). For both (a) and (b), $C = 100$, $\mu = 1$, and the detunings are $\Theta = 0$, $a = 0$, $\alpha \sim \infty$ (input field turns off infinitely fast). (a) $\Delta = 0$, (b) $\Delta = 2$.

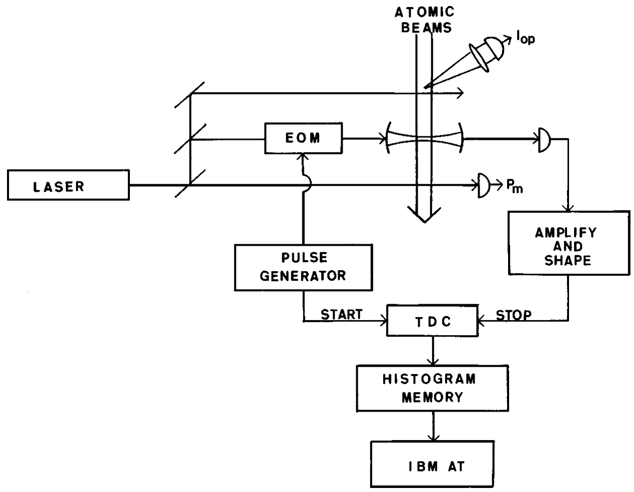

Fig. 6. Schematic of the experiment. The main components for the experiments described in the text are the electro-optic modulator (EOM), which is used to turn the input field from one level to another. It is driven by a pulse generator, which also triggers the photon-counting system. The time-to-digital converter (TDC) collects the data in the form of standardized pulses originating at the photodetector and stores it in the histogramming memory unit, from which it can later be read by the PC. The atomic beams cross the cavity waist perpendicularly as shown.

present at the time of the first emission peak. Because y_1 and the polarization field are shifted in phase by π, the size of the first peak is greatly reduced. (2) For $\sqrt{\mu C} \gg a \sim 1$, the field y decays on a time scale comparable with the dissipative time scale. The oscillatory regression is lost or the system moves to a regime of adiabatic response to the change of the driving field ($a \ll 1$).

In Fig. 3 we consider the effect of a nonzero switching ratio $\alpha \equiv y_2/y_1$, which is of a switching from an initial value y_1 to a final value $y_2 \neq 0$. For increasing α, we see a drastic decrease in the size of the oscillatory waveforms relative to the $\alpha = 0$ case. The large emission expected from the stored excitation in the atomic polarization combines out of phase with the field y left standing in the cavity to produce a greatly reduced resultant.

Figure 4 illustrates the role of cavity detuning for fixed cooperativity parameter C and atomic detuning $\Delta = 0$. For large Θ, the oscillation frequency approaches $\kappa\Theta$, corresponding to the cavity detuning. In Fig. 5 the atomic detuning Δ is varied for fixed (C, Θ). In this case the occurrence of an imaginary term in the eigenvalues corresponds to the usual splitting $\gamma_\perp\Delta$ found for an atom in free space driven by a weak, detuned field. We note in passing that the shift in response frequency Ω as one moves from the case $\Delta = 0 = \Theta$ to the case $\Theta \gg 1$ represents a cooperative analog to the vacuum radiative level shift reported in Ref. 28. This behavior in the limits of large detunings and the connection to other cavity QED systems was explored more fully in Ref. 15. Even more recently, the work of Ref. 29 looks at cavity QED effects for very large detunings $\Delta \gg 1$.

3. EXPERIMENTAL RESULTS

Our experimental apparatus is shown in Fig. 6. It consists of a set of 10 well-collimated, optically prepumped atomic beams of sodium with a rectangular cross section 0.5 mm × 2 mm (width × height). Center-to-center spacing of the beams is 1.5 mm and each has a divergence of ±1 mrad. Atoms are prepared in the $3\,^2S_{1/2}$, $F = 2$, $m_F = 2$ ground state by optical pumping with circularly polarized light to the $3\,^2P_{3/2}$, $F = 3$ state of the D_2 line at 589 nm. The two-state transition is then $3\,^2S_{1/2}$, $F = 2$, $m_F = 2$ to $3\,^2P_{3/2}$, $F = 3$, $m_F = 3$. The measured absorption width of 13 MHz is greater than the 10-MHz natural linewidth primarily because of transit broadening. For weak fields $x \ll 1$, this mechanism is modeled as a homogenous process,[30] changing the polarization decay rate $\gamma_\perp/2\pi$ from the purely radiative value of 5 MHz to 6.25 MHz. Hence $\Gamma = 0.8$, and the saturation intensity I_s for the atomic transition becomes 7.3 mW/cm^2 rather than 6.4 mW/cm^2 when $\Gamma = 1$. To draw a connection to recent work with small numbers of atoms in an optical cavity,[17,21] the single-atom cooperativity parameter for this system is $C_1 \sim 1.5 \times 10^{-2}$. The atomic beams intersect at 90°, the axis of a standing-wave cavity formed by a pair of mirrors of radius of curvature 5 cm at confocal spacing. Relevant parameters for this cavity are the mode waist $\omega_0 = 69\ \mu$m, mirror trans-

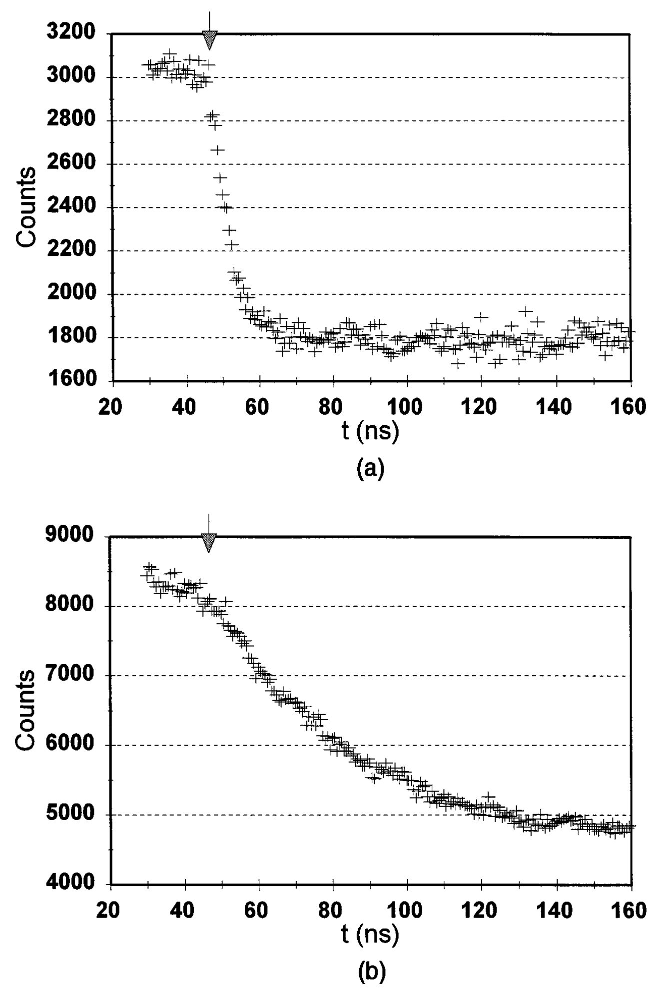

Fig. 7. Data taken by the use of the setup described in the text: (a) the input laser pulse, as recorded with neither atoms nor cavity present, (b) the transmission of the empty cavity, tuned to resonance. $\tau = 0$, the point at which the input field was switched, is marked on each of the figures by the arrow at ~45 ns.

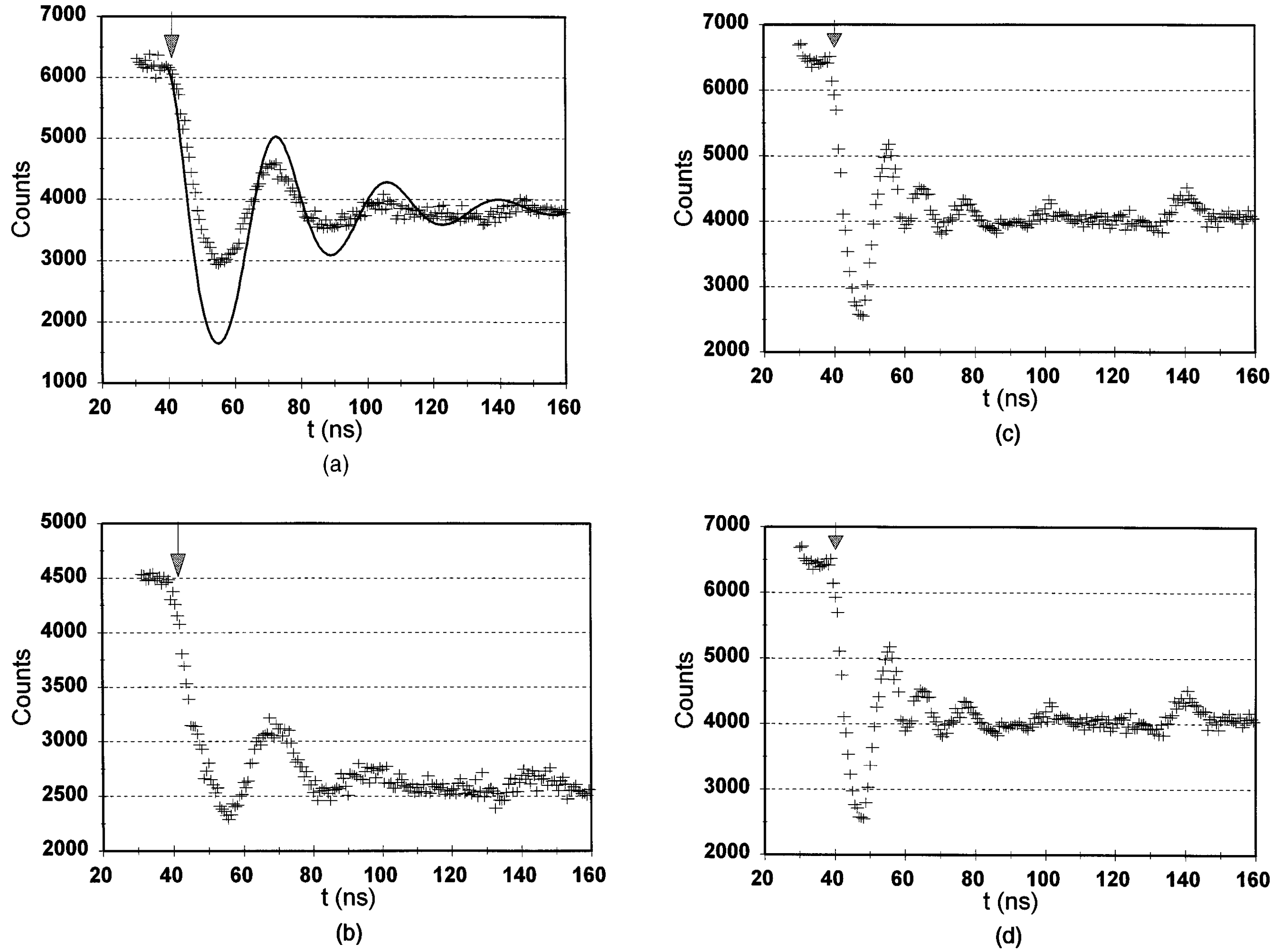

Fig. 8. Raw data for the number of counts observed per time interval of 0.625 ns, as recorded by the photon-counting electronics, with both atoms and cavity present. Common parameters for all traces are $\mu = 0.75$, $a = 2.7$, and $\alpha = 0.81$. The detunings are held close to 0 as well. Measured values of C are (a) $C \sim 10$, (b) $C = 51 \pm 11$, (c) $C = 73 \pm 12$, (d) $C = 130 \pm 20$.

mission coefficients $T_1 = T_2 = (3.0 \pm 0.1) \times 10^{-3}$, finesse $\mathcal{F} = 400 \pm 20$, and peak transmission $T_0 = 0.14 \pm 0.02$. From the cavity linewidth we calculate the parameter $\mu(\equiv 2\kappa/\gamma) = 0.750 \pm 0.038$. The excitation source is a commercial (Coherent 699-21) frequency-stabilized cw dye laser (rms linewidth 500 kHz), which is mode matched to the TEM_{00} mode of the cavity with an efficiency of greater than 94%.

After alignment to ensure perpendicularity of the excitation laser with the atomic beams (± 1 mrad), calibrations of the small-signal absorption are performed and related to the optical-pumping fluorescence and to another weak-field absorption signal measured downstream from the cavity.

The laser frequency is locked to the peak of the optical-pumping fluorescence signal. The cavity is locked to resonance by an auxiliary frequency-tunable, Zeeman-stabilized He–Ne laser whose light is double passed through an acousto-optic modulator. The red He–Ne beam enters the resonator parallel to the excitation laser, but is displaced vertically to form a ring cavity and to be spatially separated from the output signal.

As discussed above, we wish to probe the linear response of the system and thus require weak intracavity fields ($x \ll 1$). In the experiment the input intensity is switched from an initial level that satisfies the weak-field constraint to a lower level, and the time dependence of the intensity transmitted through the cavity is monitored by a standard time-correlated single-photon-counting technique.

A LeCroy 4204 time-to-digital converter records the relative time between a trigger (start) pulse edge, which is synchronous with the edge of the pulse that drives the electro-optic modulator, and an arriving nuclear instrumentation module level pulse from a constant fraction discriminator, which is the result of a detected photon. Total detection efficiency, including collection of the cavity output, quantum efficiency of the photomultiplier tube, and constant fraction discriminator threshold setting, is 2%.

The digitized time interval is transferred with a dead time of approximately 1 μs to a LeCroy 3588 histogramming memory unit that increments the bin for that time delay. After a run time (of duration ranging from 1 to 5 min) the data collection is stopped and the contents of the memory unit are read by CAMAC commands transmitted over the general-purpose interface bus (IEEE-488 standard) under the control of an IBM PC-AT. The data may then be displayed with the aid of various commercial software routines.

Two different sets of switching electronics were used, and the results of experiments for which these two different configurations were used are presented separately.

A. Case 1

For this experiment the electro-optic modulator and pulse generator pair allowed a repetition rate of 500 kHz. The decay time for the pulse was 6.2 ± 0.2 ns, or $a = 1.3$ in atomic lifetime units, and the off–on ratio was $\alpha = 0.8$. In this configuration, the output field consists of the transmitted input ($0.64\, I_0$) and a smaller contribution that is due to the coupled atom–cavity system response.

First we look at the result when an empty cavity is probed by using this technique, which is shown in Fig. 7(b). The exponential decay of the intensity from the cavity at a rate consistent with our known cavity linewidth of 7.5 MHz can be seen. For completeness, we shown in Fig. 7(a) the response at the detector with neither the atoms nor the cavity present when the intensity is switched between the same two levels by the same relative amount. Figure 8 shows the main experimental results of this paper. When the atoms are present in the cavity we see the oscillation in transmitted intensity at the coupling frequency $g\sqrt{N}$, which is indicative of the exchange of energy between the atoms and the cavity, starting with Fig. 8(a). As the number of atoms is increased we see the oscillation frequency increase [Figs. 8(b) and 8(c)]. Because of the relatively slow input pulse decay and the fact that the input field is not turned off completely ($\alpha = 0.8$), the pronounced increase in output intensity after the input field is switched (as seen in Fig. 1) is not evident.

As noted, the coupling depends on the number of atoms, and when a monitor fluorescence signal is calibrated to the intracavity small-signal absorption, the cooperativity parameter C is determined by the absolute knowledge of αl and the cavity finesse. We can then compare the measured frequency of oscillation with that predicted by theory for a given value of C. Figure 9 is a plot of the frequency, as measured from the separation of the first two peaks in intensity, versus the calculated frequency Ω_{th}. Uncertainties in the measured splitting are ±20% and ±10% for the calculated frequency. They should be equal and, within our uncertainties, this is the case, although there appears to be a systematic deviation in the slope of the curve for higher values of C.

As anomalous feature of the data is a bump that appears in all the data sets near $t = 145$ ns. This excess of counts is always in the same ratio to the ambient level, independent of the number of atoms present, and occurs at the same point in time relative to the trigger pulse edge, again independent of the number of atoms. From these considerations we can be fairly certain that the bump is not associated with any atom–cavity physics.

Shown in Fig. 8 for two of the data sets are the theoretical curves (solid curves) for the relevant parameters of the experiment. For the theoretical curves, an allowance was made to choose the parameters within our experimental uncertainty so as best to fit the data. Detunings were assumed to be identically 0 for the fits shown. It is possible to include a small jitter in detuning, which also corresponds to the experimentally achievable locking of the laser frequency and thus improves the fits somewhat for all data sets. However, with so many parameters, even when keeping within the experimentally relevant ranges, the fits are really only a qualitative measure of the theoretical consistency.

B. Case 2

We now alter the switching electronics and optics to achieve a repetition rate of 4 kHz and a pulse decay time ($1/e$) of 3.5 ± 0.5 ns, which gives a scaled decay time of $a = 2.2$. For this set of data an important difference is that the off–on ratio for the field is much greater, $\alpha = 0.2$. This corresponds more closely to the ideal situation discussed in Section 2 and illustrated in Fig. 1. The data shown in Fig. 10 clearly display the effect of the large out-of-phase polarization as it releases energy to the cavity. Figure 10 demonstrates the effect of increasing numbers of atoms present in the interaction volume of the cavity which thereby dramatically increases the effective coupling coefficients $g\sqrt{N}$. The exchange frequency is not the most dramatically changing feature; rather, one sees that the value of the output field immediately after the input is switched begins to grow rapidly following an initial decay. As explained in Section 2, this is because the polarization field emitted by the atoms is out of phase with the input field. When the input field is suddenly and greatly reduced, the polarization oscillator has no way of adjusting to the new field until a time of the order of the inverse of the polarization decay rate. Thus the opposing push of the polarization field finds itself with nothing against which it can react, and we see a net field at the output of the cavity that is much larger than the steady state. As the number of atoms is increased, the excess of the transmitted field above the steady-state field becomes larger as the square of the parameter C. For the largest number of atoms [Fig. 10(d)] we observe nearly a factor of 10 increase in the intensity transmitted by the cavity

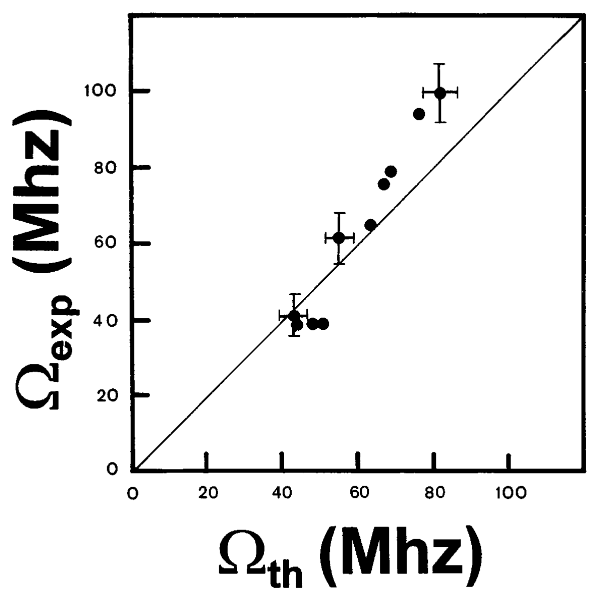

Fig. 9. Observed oscillation frequency Ω_{exp} versus theoretical prediction Ω_{th}. The frequency is the inverse of the period determined from the data of Fig. 8. The theoretical value is calculated from the value of the parameter C, which in turn was from a calibrated fluorescence signal.

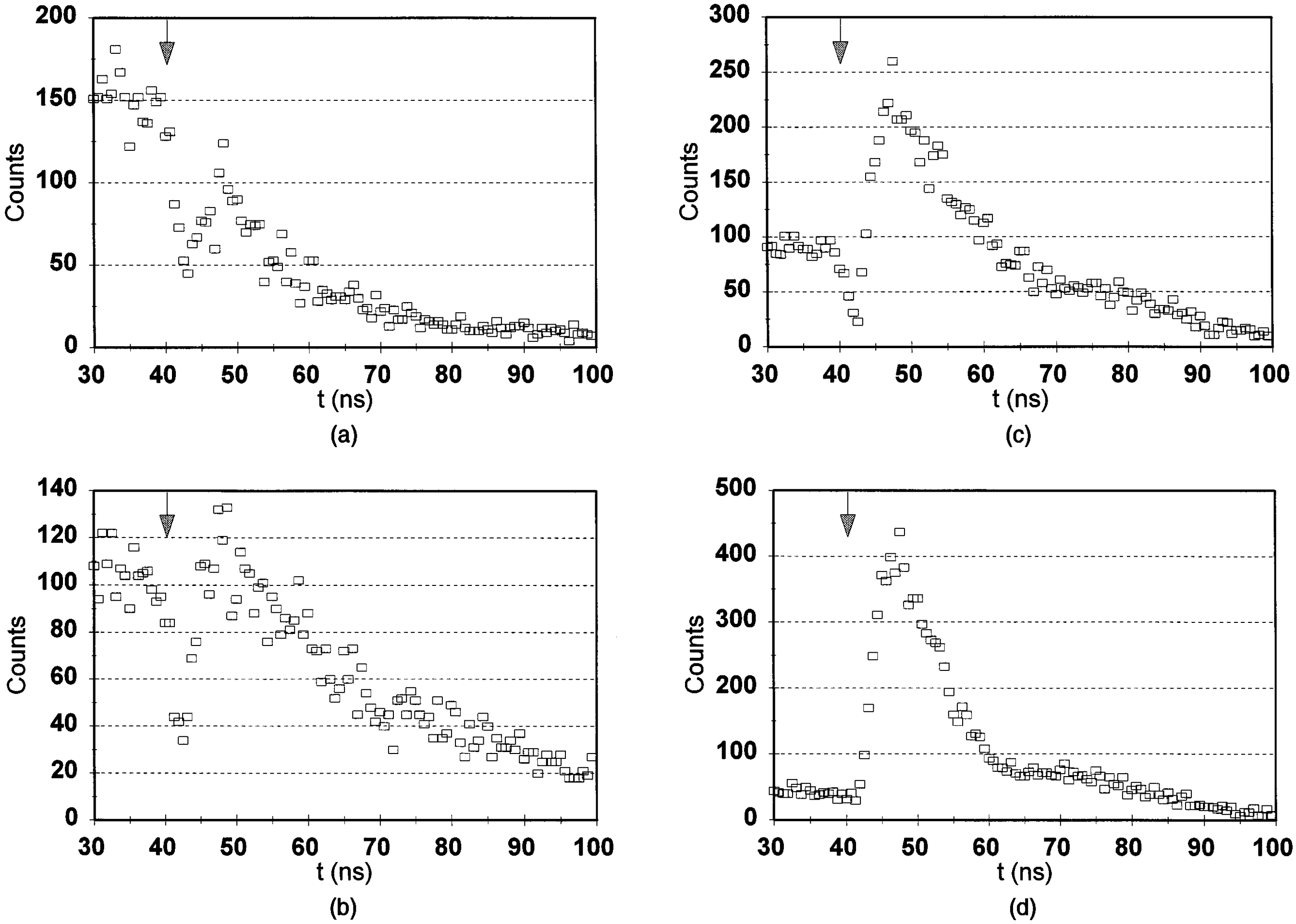

Fig. 10. Data from the second experimental configuration for which the input field was turned off more completely. Common parameters for all traces are $\mu = 0.75$, $a = 4.5$, and $\alpha = 0.2$. The detunings are held close to 0 as well. Measured values of the cooperativity parameter C are (a) $C = 29 \pm 7$, (b) $C = 50 \pm 23$, (c) $C = 101 \pm 23$, (d) $C = 175 \pm 37$. The input field switching (indicated by the arrow) occurs at ~37 ns.

after the input intensity is decreased by approximately the same factor. This is a dramatic demonstration of the concept of the darkness wave radiated by the atomic polarization. The initial decrease in output intensity seen in the first four parts of Fig. 10 is less visible as the number of atoms is increased because it becomes too fast for the resolution of the time-to-digital converter configuration; in addition it becomes washed out because of any jitter in the triggering pulses or if there are detunings that change slightly during the course of a run. In spite of this we find that the scaling of the peak height as a function of the number of atoms is roughly as it should be according to theory. In Fig. 11 the peak height is plotted as a function of the square of the cooperativity parameter. There are large error bars on this set of data, but we see that the expected C^2 dependence is borne out by the data. For this plot we have used all runs that were made under the described experimental conditions.

We have not attempted to construct a plot similar to Fig. 9 for these data, as there is at most one oscillation observed. As mentioned above, the height of the initial peak is very sensitive to the cavity and atomic detunings. One can calculate from Eq. (6) representative curves from values of our experimental parameters to demonstrate this effect. The results would be similar to those in Fig. 5. These are meant to explain qualitatively the reduction in peak height from its theoretical value with no detunings. A more realistic approach to modeling the observed behavior would include an averag-

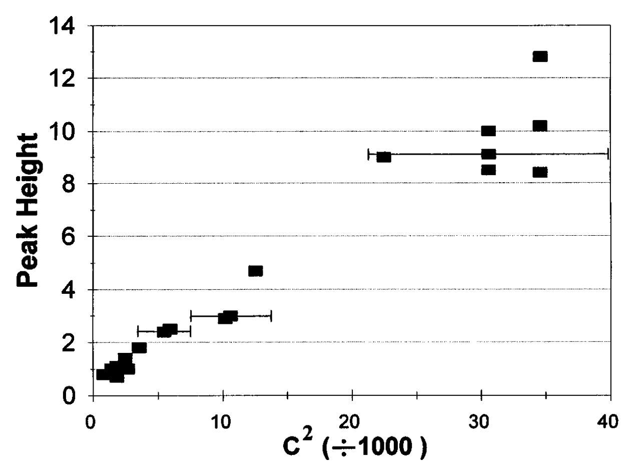

Fig. 11. Plot of the peak height versus the square of the cooperativity parameter, with data from the second experimental configuration. Experimental parameters are $\mu = 0.75$, $a = 4.5$, and $\alpha = 0.2$.

ing over different (small) detunings to simulate any jitter present in the actual experiment and to account for the smearing out of the peaks in this set of experiments.

4. CONCLUSION

We have experimentally demonstrated the oscillatory exchange of excitation between atoms and a single electromagnetic-field mode in an optical cavity. This so-called vacuum-field Rabi frequency can be explained in terms of the coupling of harmonic oscillators of similar decay rates. Our results agree with the theoretical calculations we have presented here, in which we have taken into account various nonideal experimental parameters.

Although we have taken advantage of a large number of atoms to increase the effective coupling between the cavity field and the atoms, it is important to bear in mind that the results described here are no different fundamentally from those predicted for a single atom strongly coupled to a cavity, as has been illustrated in Refs. 15 and 17.

We stress as well the agreement between theory and experiment. The simple semiclassical treatment used for the theoretical curves was used with no free parameters to fit the data, as shown in Fig. 9. Absolute values of parameters known from independent measurements were used to generate the fits to the data.

Recently studies of a related phenomenon have been carried out by several groups.[30,31,32] In semiconductor microcavities there can be an exchange of energy between the field in the cavity and the collective polarization associated with excitons. Experiments have been done in both the time and the frequency domains, as was the case with the atom–cavity system. These extensions of the vacuum Rabi oscillation concept confirm the universal nature of this coupled oscillator picture.

*Present address, Department of Physics, University of Dayton, Dayton, Ohio 45469-2314.

†Present address, Department of Physics, SUNY-Stony Brook, Stony Brook, New York 11794-3800.

‡Present address, Department of Physics, University of Arkansas, Fayetteville, Arkansas 72701.

§Present address, Norman Bridge Laboratory of Physics 12-33, California Institute of Technology, Pasadena, California 91125.

REFERENCES

1. P. Meystre, "Cavity quantum optics and the quantum measurement process," in *Progress in Optics*, E. Wolf, ed. (North-Holland, Amsterdam, 1992), Vol. XXX, pp. 261–355.
2. E. A. Hinds, "Cavity quantum electrodynamics," in *Advances in Atomic and Molecular Physics*, B. Bederson, ed. (Academic, New York, 1991), Vol. 28, pp. 271–289.
3. S. Haroche, "Cavity quantum electrodynamics," in *Fundamental Systems in Quantum Optics*, Les Houches Session LIII, J. Dalibard, J. M. Raimond and J. Zinn-Justin, eds. (Elsevier, New York, 1991), pp. 767–940.
4. P. Berman, ed., *Cavity Quantum Electrodynamics*, Supplement 2 of Advances in Atomic, Molecular and Optical Physics series (Academic, San Diego, Calif., 1994).
5. Y. Kaluzny, P. Goy, M. Gross, J. M. Raimond, and S. Haroche, "Observation of self-induced Rabi oscillations in two-level atoms excited inside a resonant cavity: the ringing regime of superradiance," Phys. Rev. Lett. **51,** 1175–1178 (1983).
6. M. Brune, J. M. Raimond, P. Goy, L. Davidovich, and S. Haroche, "Realization of a two-photon maser oscillator," Phys. Rev. Lett. **59,** 1899–1902 (1987).
7. D. Meschede, H. Walther, and G. Müller, "One-atom maser," Phys. Rev. Lett. **54,** 551–554 (1987).
8. G. Rempe, F. Schmidt-Kaler, and H. Walther, "Observation of sub-Poissonian photon statistics in a micromaser," Phys. Rev. Lett. **64,** 2783–2786 (1990).
9. G. Rempe, H. Walther, and N. Klein, "Observation of quantum collapse and revival in a one-atom maser," Phys. Rev. Lett. **58,** 353–356 (1987).
10. R. J. Brecha, L. A. Orozco, M. G. Raizen, M. Xiao, and H. J. Kimble, "Mode splitting for two-level atoms inside an optical resonator," J. Opt. Soc. Am. B **3,** 238 (1986); R. J. Brecha, L. A. Orozco, M. G. Raizen, M. Xiao, and H. J. Kimble, Bull. Am. Phys. Soc. **31,** 1973 (1986).
11. L. A. Orozco, "Optical bistability with two-level atoms," Ph.D. dissertation (University of Texas, Austin, Tex., 1987).
12. R. J. Brecha, "Nonclassical photon correlations from two-level atoms," Ph.D. dissertation (University of Texas, Austin, Tex., 1990).
13. H. J. Kimble, "Structure and dynamics in cavity-quantum electrodynamics" in Ref. 4, pp. 203–265.
14. M. G. Raizen, R. J. Thompson, R. J. Brecha, H. J. Kimble, and H. J. Carmichael, "Normal-mode splitting and linewidth averaging for two-state atoms in an optical cavity," Phys. Rev. Lett. **63,** 240–243 (1989).
15. M. G. Raizen, "Squeezing and spectroscopy of two-level atoms in a cavity," Ph.D. dissertation (University of Texas, Austin, Tex., 1990).
16. R. J. Thompson, G. Rempe, and H. J. Kimble, "Observation of normal-mode splitting for an atom in an optical cavity," Phys. Rev. Lett. **68,** 1132–1135 (1992).
17. M. G. Raizen, L. A. Orozco, M. Xiao, T. L. Boyd, and H. J. Kimble, "Squeezed-state generation by normal modes of a coupled system," Phys. Rev. Lett. **59,** 198–201 (1987).
18. L. A. Orozco, M. G. Raizen, M. Xiao, R. J. Brecha, and H. J. Kimble, "Squeezed-state generation in optical bistability," J. Opt. Soc. Am. B **4,** 1490–1500 (1987).
19. Y. Zhu, D. J. Gauthier, S. E. Morin, Q. Wu, H. J. Carmichael, and T. W. Mossberg, "Vacuum Rabi splitting as a feature of linear dispersion theory: analysis and experimental observations," Phys. Rev. Lett. **64,** 2499 (1990).
20. G. Rempe, R. J. Thompson, R. J. Brecha, W. D. Lee, and H. J. Kimble, "Optical bistability and photon statistics in cavity quantum electrodynamics," Phys. Rev. Lett. **67,** 1727–1730 (1991).
21. L. A. Lugiato, "Theory of optical bistability," in *Progress in Optics*, E. Wolf, ed. (North-Holland, Amsterdam, 1984), Vol. XXI, pp. 69–216.
22. H. J. Carmichael, "Theory of quantum fluctuations in optical bistability," in *Frontiers in Quantum Optics*, E. R. Pike, ed. (Hilger, Bristol, 1986), pp. 120–203.
23. P. D. Drummond, C. W. Gardiner, and D. F. Walls, "Quasiprobability methods for nonlinear chemical and optical systems," Phys. Rev. A **24,** 914–926 (1981).
24. E. M. Purcell, "Spontaneous emission probabilities at radio frequencies," Phys. Rev. **69,** 681 (1946).
25. M. Xiao, "Quantum fluctuations in nonlinear optics," Ph.D. dissertation (University of Texas, Austin, Tex., 1988).
26. D. Z. Anderson, J. C. Frisch, and C. S. Masser, "Mirror reflectometer based on optical cavity decay time," Appl. Opt. **23,** 1238–1245 (1984).
27. D. J. Heinzen and M. S. Feld, "Vacuum radiative level shift and spontaneous-emission linewidth of an atom in an optical resonator," Phys. Rev. Lett. **59,** 2623–2626 (1987).
28. M. Brune, P. Nussenzveig, F. Schmidt-Kaler, F. Bernardot, A. Maali, J. M. Raimond, and S. Haroche, "From Lamb shifts to light shifts: vacuum and subphoton cavity fields measured by atomic phase-sensitive detection," Phys. Rev. Lett. **72,** 3339–3342 (1994).
29. A. T. Rosenberger, L. A. Orozco, H. J. Kimble, and P. D. Drummond, "Absorptive optical bistability in two-state atoms," Phys. Rev. A **43,** 6284–6302 (1991).
30. C. Weisbuch, M. Nishioka, A. Ishikawa, and Y. Arakawa, "Observation of the coupled exciton-polariton mode splitting

in a semiconductor quantum microcavity," Phys. Rev. Lett. **69,** 3314–3317 (1992).

31. J.-K. Rhee, T. B. Norris, Y. Arakawa, M. Nishioka, and C. Weisbuch, "Time-resolved study of vacuum-Rabi oscillations in a semiconductor microcavity," in *International Quantum Electronics Conference*, Vol. 9 of 1994 OSA Technical Digest Series (Optical Society of America, Washington, D.C., 1994), paper QThE2.
32. J. M. Jacobson, H. Cao, S. Pau, G. Björk, and Y. Yamamoto, "Direct time-domain observation of microcavity exciton-polariton emission," in *International Quantum Electronics Conference*, Vol. 9 of 1994 OSA Technical Digest Series (Optical Society of America, Washington, D.C., 1994), paper QPD21.